Journal of Engineering Sciences

Vol 11, Issue 6,June/2020
ISSN NO:0377-9254

A Comparative Study of Turbulence Models on Aerodynamics Characteristics of a Fsae race car

Kathan Parekh[1], Umang Patdiwala[2]

[1]B. Tech Student, Mechanical Department, Indus University, India

[2]Assistant Professor, Mechanical Department, Indus University, India

***Abstract*— The reduction of energy consumption and drag of fsae race cars is often a serious design objective. Investigations suggest that reducing aerodynamic drags may be a more efficient method in achieving the performance desired. Accurate simulation of flow around a bluff body is extremely challenging due to the complex flow conditions around it, such as complex flow separation and laminar to turbulent flow transition. This paper investigates the flow over a fsae race car. Four popular turbulence models, like the Spalart-Allmaras, Realizable k-ε, SST k-ω and Reynolds Stress equation models are studied. The objective of this study is to compare the performances of these models in simulating such a category of flows. With properly generated mesh and discretization schemes, the RANS approach is able to capture the prominent features of the extremely complex flow. The performance is as good as the LES solvers, especially for steady-state flow simulations. The k-ω SST model produces the best results among the three models studied. This study could assist designers in the fsae competition and automotive industry in the applications of these cost-effective tools to improve their design productivity. Future study will focus on the performances of the models in simulating time-dependent flows over the fsae race car.**

***Keywords*— Turbulence model; Formula SAE race car; CFD analysis; Aerodynamics; Supra.**

1. INTRODUCTION

1.1. FSAE

Formula SAE also known as Formula student is a racing competition of open wheel formula style race cars organized by SAE India at national level in which college students from different parts of the nation form a team to design and manufacture the race car while strictly following the rules provided to them. As the event is held at national level, competition is really tough and the slightest advantage can be the reason for the win. The goal of aerodynamics engineer in the team is to find the right balance between drag and down force for the car to be able to reach to the podium.

1.2. Turbulence Model

Development of drag reduction technology of a car is aided by aerodynamic shape optimization based on computational fluid dynamics (CFD), which is very much dependent on the capability to predict aerodynamic flows accurately. Aerodynamic flows are indicated by high Reynolds numbers, usually ten to one hundred million, Mach numbers ranging from low subsonic at take-off and landing to supersonic, and a combination of laminar and turbulent flow. These type of flows are usually attached or loosely separated and steady, with large-scale separation or unsteadiness present under limited circumstances, such as in coves, behind deployed spoilers, under post-stall conditions, after the onset of buffet and other off-design conditions. Prediction of aerodynamic flows requires the ability to compute phenomena such as boundary layers, wakes, confluent boundary layers, shock-boundary layer interactions, laminar-turbulent transition, transitional flows, separation points, separated flows and reattachment points. In the circumstances of aerodynamic shape optimization, given the present situation, computers and algorithms, currently there is no practical alternative to solving the Reynolds-Averaged Navier-Stokes (RANS) equations. The RANS equations involve the effects of turbulence that are generated from Reynolds stresses, which are apparent stresses that grows as a result of time averaging the Navier-Stokes equations over an interval of time which is longer than the characteristic time scales of the turbulence. Typically, some particularly difficult flow problems are identified. These function the catalyst for the

Vol 11, Issue 6,June/2020
ISSN NO:0377-9254

following generation of turbulence models, which are typically of increased complexity. the prevalence of the new models is usually demonstrated by their accuracy for these specific problems. This evolutionary process is flawed in two important respects. First, it's often possible to tune a turbulence model to realize a specific known result. Therefore, it's insufficient to demonstrate that a model is more accurate for a specific problem without showing that accuracy appreciate or better than that of the previous models is maintained for a broad suite of flows. As an example, a turbulence model that produces a maximum lift coefficient that's lower and in better agreement with experiment than other models for a specific airfoil may produce a maximum lift coefficient that's too low for other airfoils that the opposite models are accurate. Second, the flow problem that inaccurate comparisons with experiment are obtained is also difficult for reasons unrelated to the turbulence model. It might be that the experimental data are flawed. As an example, a purportedly two-dimensional data set could even have three-dimensional features, thus causing the discrepancies assumed to be the results of an inadequate turbulence model. There are several possible reasons for disagreement between theory and experiment aside from the turbulence model, as further discussed below. The target of the current article is to supply a perspective on turbulence modelling for aerodynamic flows supported the authors' combined thirty 30 years of experience solving such flows. As such, we don't provide a comprehensive overview of accessible turbulence models. Our goal is to produce some thoughts relevant to the selection of a turbulence model and a few future research directions, instead of recommending a specific model.

2. Theory

2.1. RANS

RANS or Reynolds averaged Navier-Stokes is a turbulence modelling equation. This approach to turbulence modelling requires that Reynolds stresses are properly modeled. The Boussinesq hypothesis is used in S-A, k-ε and k-ω models.

$$-\rho\overline{u_i'u_j'}=\mu_t\left(\frac{\partial u_i}{\partial x_j}+\frac{\partial u_j}{\partial x_i}\right)-\frac{2}{3}\left(\rho k+\mu_t\frac{\partial u_k}{\partial x_k}\right)\delta_{ij} \qquad (1)$$

2.2. Spalart-Allmaras

The transported variable within the Spalart-Allmaras model, v, is just like the turbulent kinematic viscosity except in the near-wall (viscosity-affected) region. The transport equation for the modified turbulent viscosity is,

$$\frac{\partial}{\partial t}(\rho\tilde{\nu})+\frac{\partial}{\partial x_i}(\rho\tilde{\nu}u_i)=G_\nu+\frac{1}{\sigma_{\tilde{\nu}}}\left[\frac{\partial}{\partial x_j}\left\{(\mu+\rho\tilde{\nu})\frac{\partial\tilde{\nu}}{\partial x_j}\right\}+C_{b2}\rho\left(\frac{\partial\tilde{\nu}}{\partial x_j}\right)^2\right]-Y_\nu+S_{\tilde{\nu}}$$

[1](2)

where is that the production of turbulent viscosity, and is that the destruction of turbulent viscosity that happens within the near-wall region thanks to wall blocking and viscous damping, and are the constants and is the molecular kinematic viscosity. is a user-defined source term. Since the turbulence kinetic energy, v, is not calculated in the Spalart-Allmaras model, the last term is ignored when estimating the Reynolds stresses.

2.3. Realizable k-ε

The turbulence kinetic energy, k, and its rate of dissipation, ε, are obtained from equation,

$$\frac{\partial}{\partial t}(\rho k)+\frac{\partial}{\partial x_i}(\rho k u_i)=\frac{\partial}{\partial x_j}\left[\left(\mu+\frac{\mu_t}{\sigma_k}\right)\frac{\partial k}{\partial x_j}\right]+G_k+G_b-\rho\epsilon-Y_M+S_k$$

and

$$\frac{\partial}{\partial t}(\rho\epsilon)+\frac{\partial}{\partial x_i}(\rho\epsilon u_i)=\frac{\partial}{\partial x_j}\left[\left(\mu+\frac{\mu_t}{\sigma_\epsilon}\right)\frac{\partial\epsilon}{\partial x_j}\right]+C_{1\epsilon}\frac{\epsilon}{k}(G_k+C_{3\epsilon}G_b)-C_{2\epsilon}\rho\frac{\epsilon^2}{k}+S_\epsilon$$

(3)

2.4. SST k-ω

The turbulence kinetic energy, k, and its rate of dissipation, ω, are obtained from equation,

$$\frac{\partial}{\partial t}(\rho k)+\frac{\partial}{\partial x_i}(\rho k u_i)=\frac{\partial}{\partial x_j}\left[\Gamma_k\frac{\partial k}{\partial x_j}\right]+G_k-Y_k+S_k+G_b$$

and

$$\frac{\partial}{\partial t}(\rho\omega)+\frac{\partial}{\partial x_i}(\rho\omega u_i)=\frac{\partial}{\partial x_j}\left(\Gamma_\omega\frac{\partial\omega}{\partial x_j}\right)+G_\omega-Y_\omega+S_\omega+G_{\omega b}$$

(4)

Where, G_k represents generation of turbulence kinetic energy due to mean velocity gradients. G_ω represents the generation of ω.

2.5. Reynolds Stress

The transport Equation for the transport of Reynolds stresses is,

$$\underbrace{\frac{\partial}{\partial t}\left(\rho\overline{u_i'u_j'}\right)}_{\text{Local Time Derivative}}+\underbrace{\frac{\partial}{\partial x_k}\left(\rho u_k\overline{u_i'u_j'}\right)}_{C_{ij}\equiv\text{Convection}}=\underbrace{-\frac{\partial}{\partial x_k}\left[\rho\overline{u_i'u_j'u_k'}+\overline{p'\left(\delta_{kj}u_i'+\delta_{ik}u_j'\right)}\right]}_{D_{T,ij}\equiv\text{Turbulent Diffusion}}$$

(5)[3]

3. Method

Design of the car was done in Solidworks, which was then imported into Ansys Fluent to carry out cfd simulations. Cfd study was carried out on the same model using the four selected models,

Vol 11, Issue 6,June/2020
ISSN NO:0377-9254

and the data was compared. Symmetry was used to help reduce computational load and time.

Parameters	Value
Velocity Inlet	30 m/s
Pressure outlet	0 gauge pressure
Symmetry plane	symmetry
Walls	0 shear stress
Body	No slip
Wheels	Rotating
Ground	Moving
Solver	Pressure based

Table 1. Solver Settings

3.1. Analysis

3d model used for simulation is shown in figure. The surface mesh as well as volume mesh are shown. The computational domain is kept sufficient enough so that there is no backward flow.

Fig. 1 Isometric view of 3d model

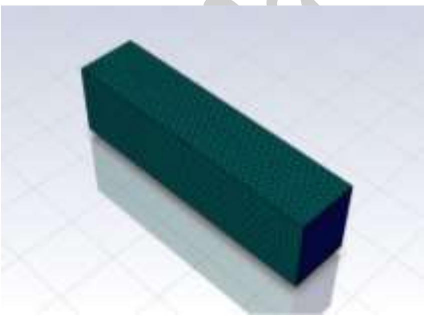

Fig. 2 Isometric view of Computational domain

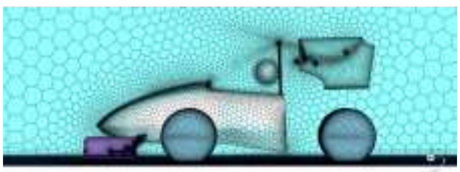

Fig. 3 Surface mesh

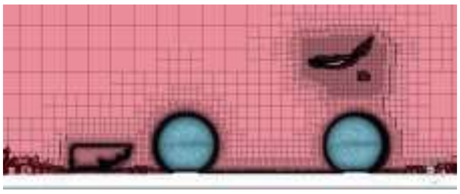

Fig. 4 Volume mesh

4. Observations

Parameter	Drag Force (N)	C_D	Lift Force (N)	C_L	Efficiency (C_L/C_D)
Body	99.795	0.181	-9.108	-0.016	-0.088
Front wheels	6.231	0.011	15.964	0.028	2.545
Front wing	74.411	0.134	-512.369	-0.929	-7.115
Rear wheels	22.587	0.040	35.406	0.061	1.525
Rear wing	145.013	0.263	-633.648	-1.149	-4.368

Table 2. Result of Car Model using Spalart-Allmaras

Parameter	Drag Force (N)
Body	99.480
Front wheels	5.743
Front wing	76.592
Rear wheels	33.252
Rear wing	138.042

Vol 11, Issue 6,June/2020
ISSN NO:0377-9254

C_D	Lift Force (N)	C_L	Efficiency (C_L/C_D)
0.180	-10.002	-0.018	-0.100
0.010	15.744	0.028	2.800
0.138	-540.080	-0.979	-7.094
0.060	27.922	0.050	0.833
0.250	-618.261	-1.121	-4.484

Table 3. Result of Car Model using Realizable k-ε

Parameter	Drag Force (N)	C_D	Lift Force (N)	C_L	Efficiency (C_L/C_D)
Body	99.108	0.179	-9.713	-0.017	-0.094
Front wheels	4.214	0.007	15.918	0.028	4.000
Front wing	75.675	0.137	-535.702	-0.971	-7.087
Rear wheels	34.107	0.061	27.022	0.049	0.803
Rear wing	138.987	0.252	-621.606	-1.127	-4.472

Table 4. Result of Car Model using SST k-ω

Parameters	Drag Force (N)	C_D	Lift Force (N)	C_L	Efficiency (C_L/C_D)
Body	98.647	0.178	-6.972	-0.012	-0.067
Front wheels	5.324	0.009	15.628	0.028	3.111
Front wing	76.072	0.137	-537.334	-0.974	-7.109
Rear wheels	31.690	0.057	29.596	0.053	0.929
Rear wing	141.567	0.256	-624.797	-1.133	-4.425

Table 5. Result of Car Model using Reynolds Stress equation

From table 2-5, we can observe that there is not much difference in the values of forces obtained from the different. This can be due to the reason that every model is very accurate in predicting the values and also that they are constantly modified and kept up to date. Reynolds stress equation model being a 7-equation model takes the longest to converge, and also gives more data compared to the other three which are only 2 equation models.

4.1. Velocity cut plots

From fig. 5-8, we can see that there are no major differences visible in the contours of velocity, there is only a minor difference in the max velocity of the models.

Journal of Engineering Sciences

Vol 11, Issue 6,June/2020
ISSN NO:0377-9254

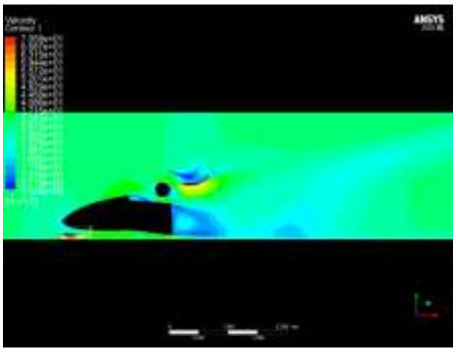

Fig. 5 Velocity cut plot of Spalart-Allmaras case

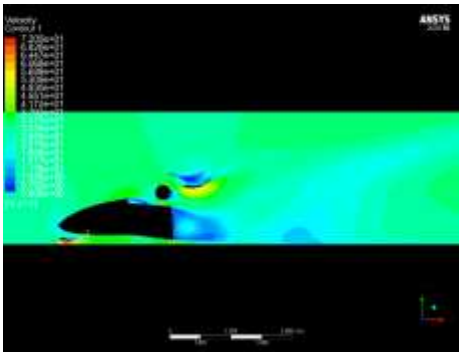

Fig. 6 Velocity cut plot of Realizable k-ε case

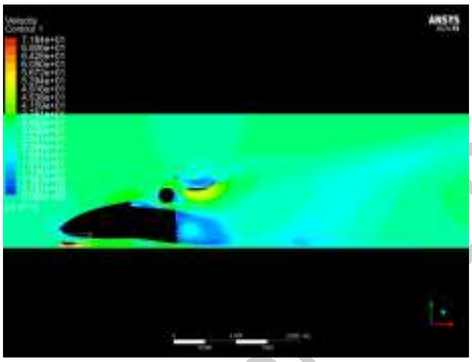

Fig. 7 Velocity cut plot of SST k-ω case

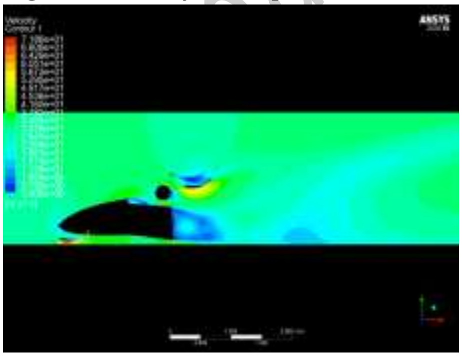

Fig. 8 Velocity cut plot of Reynolds Stress case

4.2. Pressure cut plots

From fig. 9-12, we can see that there are some differences visible in the contours of pressure, there is only a minor difference in the max pressure of the models. The wake structure created at the back of the vehicle is different in every case and is clearly seen.

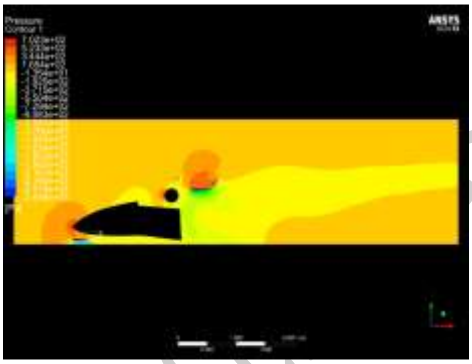

Fig. 9 Pressure cut plot of Spalart-Allmaras case

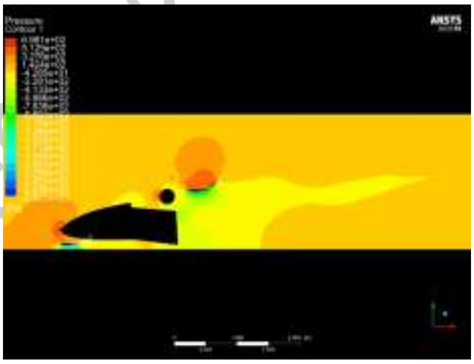

Fig. 10 Pressure cut plot of Realizable k-ε case

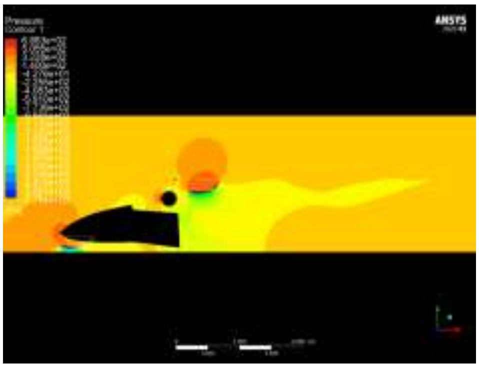

Fig. 11 Pressure cut plot of SST k-ω case

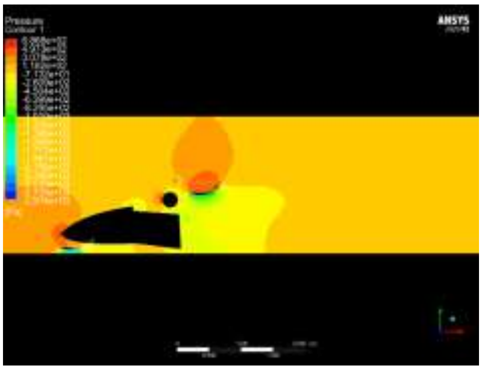

Fig. 12 Pressure cut plot of Reynolds Stress case

4.3. Velocity streamlines

From fig. 13-20, we can see that there are some differences visible in the streamlines, flow around the car id=s observed. The wake structure created at the back of the vehicle is again different in every case and is clearly seen.

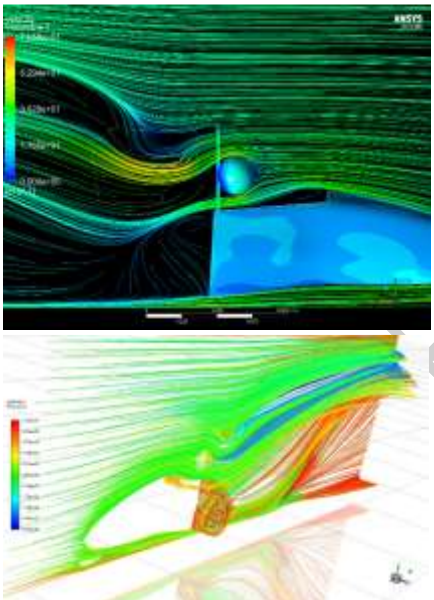

Fig. 13,14 Streamlines of Spalart-Allmaras case

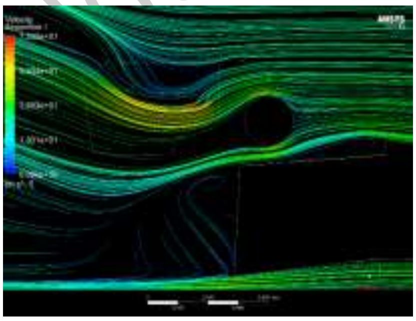

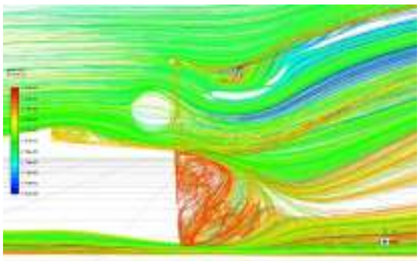

Fig. 15,16 Streamlines of Realizable k-ε case

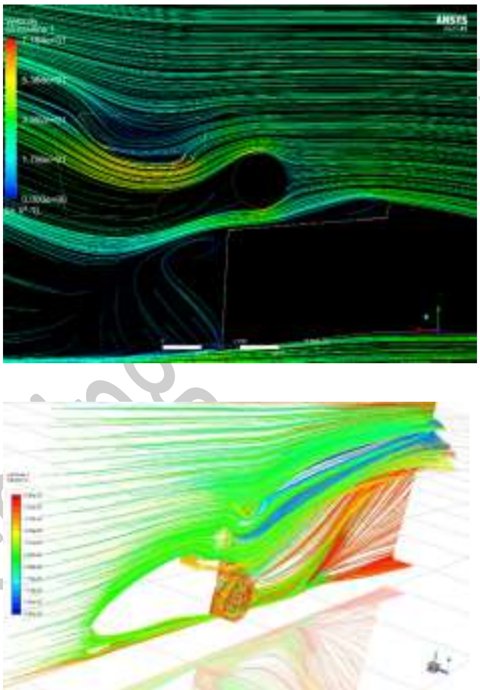

Fig. 17,18 Streamlines of SST k-ω case

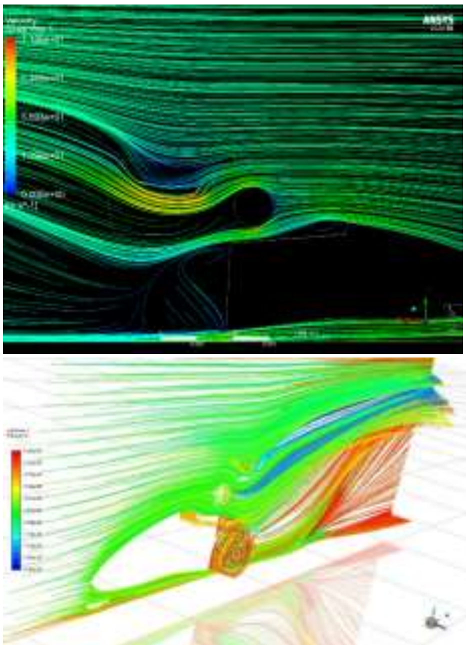

Fig. 19,20 Streamlines of Reynolds Stress case

Journal of Engineering Sciences
Vol 11, Issue 6,June/2020
ISSN NO:0377-9254

4.3. Wake

Fig. 21-25 shows the wake from behind, which is nearly identical in every case.

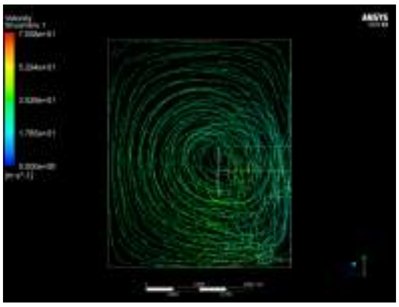

Fig. 21 Wake created in Spalart-Allmaras case

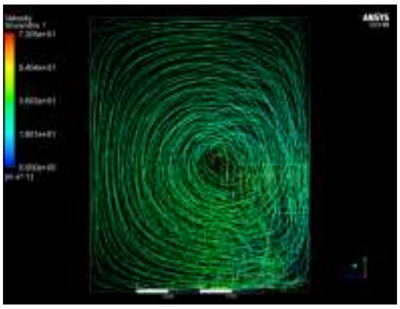

Fig. 22 Wake created in Realizable k-ε case

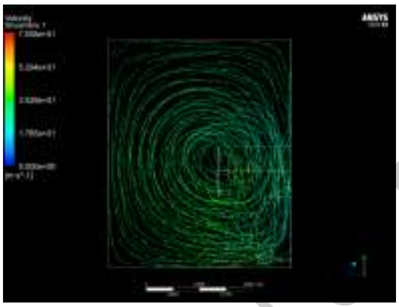

Fig. 23 Wake created in SST k-ω case

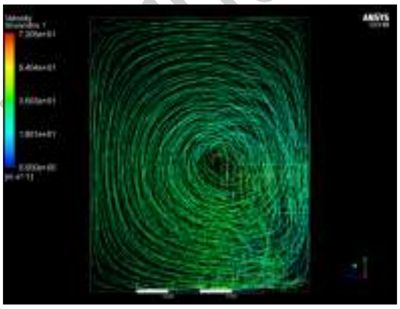

Fig. 24 Wake created in Reynolds Stress case

4.4. Wall y+

Fig. 25-28 shows the y+ value on the body, this just shows that the meshing and the prism layers added are proper and the u and y values achieved are correct.

Fig. 25 Wall y+ of Spalart-Allmaras case

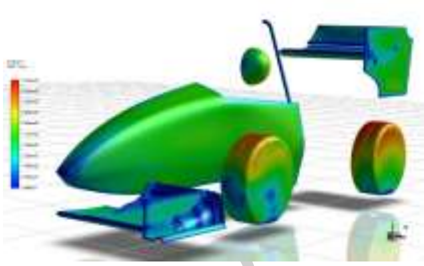

Fig. 26 Wall y+ of Realizable k-ε case

Fig. 27 Wall y+ of SST k-ω case

Fig. 28 Wall y+ of Reynolds Stress case

Vol 11, Issue 6,June/2020
ISSN NO:0377-9254

5. Results

Model type	Spalart-Allmaras	Realizable k-ε	SST k-ω	Reynolds Stress
Drag Force(N)	350.407	353.112	352.093	353.302
C_D	0.635	0.640	0.638	0.640
Lift Force	-1082.759	-1224.678	-1124.081	-1123.880
C_L	-1.964	-2.040	-2.039	-2.038
Efficiency (C_L /C_D)	-3.092	-3.187	-3.195	-3.184

Table 6. Result of Analysis

Turbulence Model	Spalart-Allmaras	Realizable k-ε	SST k-ω	Reynolds Stress
Pressure (Pa)	672.497	698.102	667.667	674.474
Velocity (m/s)	66.510	72.151	67.732	67.747
Iterations to converge	100	250	390	500

Table 7. Result of Analysis

From the compilation of all the data, we can get a clear idea of exactly how different each model is and how it predicts the values. Values of all the cases are almost identical, the simulation was run until convergence was reached. The major difference seen is in the number of iterations required to reach convergence.

6. Conclusion

This paper studies aerodynamic characteristic of fsae race car using four different turbulence models, to obtain pressure and velocity values and also to obtain the flow around the car. All the four cases were compared and following conclusions were drawn. All the models have evolved over the years and corrections have made to each of them to make them as perfect as possible, which is observed in this study. All the values obtained are very similar to each other, and close enough to each other so that we can say that if obtaining drag and lift value is the goal, any of these models are appropriate and accurate. If observing the airflow around the car is the objective, there are minor

Vol 11, Issue 6,June/2020
ISSN NO:0377-9254

differences observed between these four models. Reynolds stress equation model predicts the airflow closest pretty accurately, but it requires a lot of computational power, which is not readily available to students participating in the fsae competition. That is why SST k-ω is the best option as it also predicts airflow accurately, with significantly less computational power. Realizable k-ε yields the highest values out of the four. Iterations required for the simulation to converge are the main differentiating point between them. So, it can be concluded that selection of the turbulence model can be done on the basis of the availability of computational resources.

7. Future work

Future study will focus on the performances of the models in simulating time-dependent flows over the fsae race car also known as transient simulation. That requires quite a lot of computational power as well as time. But it can help predict the flow better and instantaneous values can be obtained.

REFERENCES

[1] P. R. Spalart and S. R. Allmaras, A One-Equation Turbulence Model for Aerodynamic Flows, AlAA-92-0439.

[2] Dastan Igali, Olzhas Mukhmetov, Yong Zhao, Sai Cheong Fok and Soo Lee, Comparative Analysis of Turbulence Models for Automotive Aerodynamic Simulation and Design. Doi 10.1007/s12239-019-0107-7.

[3] The ANSYS Fluent Theory Guide,2020

[4] Serre, E., Minguez, M., Pasquetti, R., Guilmineau, E., Deng, G. B., Kornhaas, M., Schäfer, M., Fröhlich, J., Hinterberger, C. and Rodi, W. (2013). On simulating the turbulent flow around the Ahmed body: A French–German collaborative evaluation of LES and DES. Computers & Fluids.

[5] O. Grundestam, S. Wallin, P. Eliasson, A. V. Johansson. Application of Reynolds Stress Models to High-Lift Aerodynamics Applications. https://doi.org/10.1016/B978-008044544-1/50058-3

[6] D. W. Zingg & P. Godin (2009): A perspective on turbulence models for aerodynamic flows, International Journal of Computational Fluid Dynamics, 23:4, 327-335. http://dx.doi.org/10.1080/10618560902776810

[7] Launder BE and Spalding DB, The numerical computation of turbulent flows. Comp. Meth. Appl. Mechanics Engr., 1974, Vol. 3, 269-89.

[8] Walters D.H. and Leylek J.H. (2003b) Simulation of Transitional Boundary-Layer Development on a Highly-Loaded Turbine Cascade with Advanced RANS Modeling, Proceedings of ASME Turbo Expo, 2003-38664.

[9] Mattias Olander, CFD Simulation of the Volvo Cars Slotted Walls Wind Tunnel Master's Thesis in Solid and Fluid Mechanics, Chalmers University of Technology, Goteborg, Swedon, 2011, 33.

[10] Menter FR, Two-Equation Eddy-Viscosity Turbulence Models for Engineering Applications. AIAA J., 1994, Vol. 32, 1598-1605.

[11] W. Kieffers, S. Moujaes and N. Ambya, CFD study of section characteristics of Formula Mazda race car wings, Mathematical and Computer Modelling, Vol.43 (11-12), 1275-1287.

[12] Oliver Fischer, Timo Kuthada, Jochen Wiedemann, Patrick Dethioux, Richa Mann and Brad Duncan, CFD validation study for a Sedan scale Model in an Open Jet Wind Tunnel, SAE International, 2008, 1-0385.

[13] Singh R. CFD Simulation of NASCAR Racing Car Aerodynamics, SAE Technical paper, 2008, 01-0659.

[14] Sneh Hetawal, Mandar gophane, Ajay B.K. and Yagnavalkya Mukkamala, Aerodynamic study of Formula SAE car, Procedia Engineering, 97, 2014, 1198 – 1207.

[15] Zhang Ying-chao and Fu Li-min, Transient aerodynamic numerical simulation of simplified shape cars under condition of opposite meet side by side in tunnel, Journal of Jilin University, 2006, 03.